Deformational-energy partitioning in glacier shear zones

Meghana Ranganathan[1], Brent Minchew[1], Colin R Meyer[2], and Matej Pec[1]

[1]Massachusetts Institute of Technology
[2]Dartmouth College

November 23, 2022

Abstract

Most of the mass loss from the Antarctic Ice Sheet occurs through glaciers and ice streams, where fast-flow is partially controlled by rapid ice deformation in the margins. Deformation drives thermomechanical and recrystallization processes that influence further deformation, a feedback which may destabilize glaciers. However, few models account for the feedback between deformation and recrystallization. We derive an idealized model for ice temperature and grain-size that partitions deformational work into dissipated heat and changes in strain and surface energy, all of which drive dynamic recrystallization. Under conditions common in glacier shear margins, we show that a large portion of deformational work is stored as elastic energy, with the remainder dissipated as heat. This result revises our current picture of the amount of heat generated in glacier shear margins and suggests that changes in internal strain through dynamic recrystallization of ice likely play an important role in facilitating fast-flowing glacial ice.

Deformational-energy partitioning in glacier shear zones

Meghana Ranganathan[1], Brent Minchew[1], Colin R. Meyer[2], Matěj Peč[1]

[1]Department of Earth, Atmospheric and Planetary Sciences, Massachusetts Institute of Technology, Cambridge, MA, USA
[2]Thayer School of Engineering, Dartmouth College, Hanover, NtH, USA

Key Points:

- Deformational work is partitioned into dissipated heat and stored strain energy, with possibly $\leq \frac{1}{2}$ of work being dissipated as heat.
- Accounting for energy partitioning leads to less heating and a larger role for recrystallization processes than previously thought.

Corresponding author: Meghana Ranganathan, `meghanar@mit.edu`

Abstract

Most of the mass loss from the Antarctic Ice Sheet occurs through glaciers and ice streams, where fast-flow is partially controlled by rapid ice deformation in the margins. Deformation drives thermomechanical and recrystallization processes that influence further deformation, a feedback which may destabilize glaciers. However, few models account for the feedback between deformation and recrystallization. We derive an idealized model for ice temperature and grain-size that partitions deformational work into dissipated heat and changes in strain and surface energy, all of which drive dynamic recrystallization. Under conditions common in glacier shear margins, we show that a large portion of deformational work is stored as elastic energy, with the remainder dissipated as heat. This result revises our current picture of the amount of heat generated in glacier shear margins and suggests that changes in internal strain through dynamic recrystallization of ice likely play an important role in facilitating fast-flowing glacial ice.

Plain Language Summary

Fast-flowing glaciers on the Antarctic Ice Sheet eject significant amounts of ice each year, contributing to global sea-level rise, and a prerequisite to projecting the future behavior of these glaciers is understanding the physical processes that occur when ice flows rapidly. Here, we estimate the energy changes that occur when ice deforms in order to determine what the dominant physical processes are. While previously, it has been assumed that when ice deforms, all the energy changes that occur drive heating, we find that fast flow and rapid deformation also drives recrystallization, which describes mechanisms that alter aspects of the physical microstructure of ice. This result suggests that heating is less significant than previously thought and that ice flow models may need to account for other processes, such as recrystallization processes, in order to effectively model changes that will occur to fast-flowing glaciers.

1 Introduction

Rapid deformation occurs in glaciers that transport significant mass to the ocean and often controls the speed at which these glaciers lose mass (Rignot, 2004; Wingham et al., 2009). Zones of significant deformation in glaciers typically occur in the lateral margins, denoted shear margins, because they are the boundaries that separate fast-flowing ice from roughly stagnant ice or rock. Deformation induces positive feedbacks that enhance flow and alter the response of glaciers to changing forcing (Echelmeyer et al., 1994; Hindmarsh, 2004; Schoof, 2004; Suckale et al., 2014; Meyer et al., 2016). Thus, accurately projecting changes to Antarctic glaciers requires a complete understanding of the physical processes activated by deformation.

The energy changes that occur during deformation obey the first law of thermodynamics:

$$\dot{U} = \dot{Q} + \dot{W} \tag{1}$$

where the overdot represents rate of change with respect to time. $\dot{U}$ is the rate of change of internal energy, $\dot{Q}$ is the rate of heat transport across the boundary of the control volume, and $\dot{W}$ is the rate of work done on the volume by the surrounding material. $\dot{U}$ is the sum of thermal energy changes within the volume and non-thermal energy changes. Thermal energy is heat and entails the vibration of molecules in a crystalline lattice (Figure 1a,i). Non-thermal energy is primarily a function of surface energy, which describes the energy associated with broken bonds along a two-dimensional surface with the maintenance of a solid lattice elsewhere (Figure 1a,ii), and elastic strain energy, which results from the translation of molecules within the lattice (Figure 1a,iii), and .

Taken together, these sources of energy describe the total internal energy. Energy components not considered in this study include latent heat of fusion and kinetic energy. The latent heat of fusion (the energy required to destroy the crystalline lattice) is not considered here because we focus this study on the dynamics of ice below its melting point. Kinetic energy describes the bulk motion of the control volume and is negligibly small due to the slow movement of glaciers. In these conditions, and assuming incompressibility, the change in internal energy is described by

$$dU = \rho c_p dT + dE_{\text{non-thermal}} \tag{2}$$

where $E_{\text{non-thermal}}$ represents non-thermal (strain and surface) energy per unit volume. Following this definition, the energy balance can be written as (full derivation in Supplement Text S1)

$$\dot{E}_{\mathrm{non-thermal}} = (1 - \Theta)\tau_{ij}\dot{\epsilon}_{ij} \tag{3}$$

$$\rho c_p \Big(\frac{\partial T}{\partial t} + \underline{\mathrm{u}} \cdot \nabla T \Big) = K \nabla^2 T + \Theta \tau_{ij} \dot{\epsilon}_{ij} \tag{4}$$

Θ is the fraction of work done during deformation that is dissipated as heat and takes a value between 0 and 1, and $\tau_{ij}\dot{\epsilon}_{ij}$ is the work done to deform the ice, $\dot{\epsilon}_{ij}$ is the strain rate tensor, and τ_{ij} is the deviatoric stress tensor. We use summation convention for repeated indices. Equation 4 is the heat equation, where c_p is the specific heat capacity for ice, T is ice temperature, $\underline{\mathrm{u}}$ is the ice velocity vector, and K is thermal conductivity which we assume is spatially constant and independent of temperature. An analogous representation using enthalpy is presented in Supplement Text S1 and treats explicitly the partitioning of enthalpy into thermal and non-thermal components.

Using Equation 4, with $\Theta = 1$, studies estimate ice temperature in zones of high shear and suggested the presence of extensive temperate zones. These studies propose a connection between meltwater formed in temperate zones with the glacial hydrologic system that may provide a significant control on the speed of fast-flowing glaciers (Perol and Rice, 2015; Meyer and Minchew, 2018; Meyer et al., 2018). Considering only the effect of heating on deformation, however, as has been the case in studies of deformation in glaciers, implicitly assumes that deformationally-induced changes to non-thermal energies are negligible.

Figure 1b shows the effect of varying Θ on temperature profiles in an idealized shear margin, wherein ice temperature is computed from a 1D thermomechanical model derived by Meyer and Minchew (2018) (Supplement Text S3). If almost all the deformational work is dissipated as heat ($\Theta \to 1$), ice temperature increases rapidly with depth. With less work going into heating and more work going into changes in non-thermal energy (decreasing Θ), ice temperatures increase with depth less rapidly, becoming approximately constant with depth as $\Theta \to 0$. To our knowledge, no study has evaluated the validity of the assumption that $\Theta = 1$ in ice. Further, constraining Θ is critical to gain an accurate representation of the thermomechanics and energetics of deforming glacial ice.

This question has been examined in experimental rock mechanics and metallurgy studies, and these studies find that work is partitioned between heat and stored energy, with amount of work going into stored energy being significant (up to 60% of the work rate). These studies also find that this partitioning varies with strain and strain-rate (Mason et al., 1994; Rosakis et al., 2000; Hodowany et al., 2000). A parameter similar to Θ has been proposed and included in models (e.g. (Rosakis et al., 2000; Austin and Evans, 2007; Behn et al., 2009)). Without a similar study and method of incorporating Θ into models, studies on ice flow in glaciers may be neglecting significant energy sources and sinks.

Changes in surface ($\dot{E}_{\text{surface}}$) and elastic strain ($\dot{E}_{\text{strain}}$) energy in response to deformation predominately occur through dynamic recrystallization, a set of mechanisms that alter the size and orientation of grains in response to deformation. These mechanisms reduce grain size by the rotation of the lattice subdividing grains, which primarily alters surface energy, and the outward migration of grain boundaries growing grains, which alters the total amount of elastic strain energy in a given volume and changes surface energy by reducing the grain boundary density (Derby and Ashby, 1987; Duval and Castelnau, 1995).

In this paper, we compute changes in surface, thermal, and strain energies, enabling estimates of Θ. To do this, we apply a steady state model that accounts for changes in grain size due to dynamic recrystallization to estimate changes in surface and elastic strain energy (Ranganathan et al., 2021). We couple this grain size model to a thermomechanical model (Meyer and Minchew, 2018), which computes changes in thermal energy. We apply this model to estimate Θ in shear margins in Pine Island Glacier in West Antarctica (and other glaciers in Supplement Text S6) to study the effect of thermally-driven feedbacks in rapidly-deforming glaciers.

2 Modeling Energy Partitioning

We find Θ by computing the fraction of changes in thermal energy to changes in total ($\dot{E}_{\text{thermal}}+\dot{E}_{\text{strain}}+\dot{E}_{\text{surface}}$) energy as ice deforms (see Supplement Text S1; Figure 1c). During deformation, the mechanical work is converted into a combination of thermal energy and strain energy, which builds up in the grains due to the formation of dislocations (Derby and Ashby, 1987; Derby, 1992; De La Chapelle et al., 1998). Thermal energy is advected and diffused (Equation 4). Strain energy, on the other hand, is not diffused. The increase in strain energy within grains reduces the rate of deformation due to work-hardening, in which pileups of dislocations reduce dislocation mobility in the lattice (Wilson and Zhang, 1996). Recrystallization mechanisms annihilate dislocations, thereby relieving this strain energy, by the outward migration of grain boundaries, which destroys dislocations in the path of the moving boundary (migration recrystallization), or by the subdivision of grains, during which new, strain-free grains are formed (rotation recrystallization) (Rollett and Kocks, 1993; Wenk et al., 1997; De Bresser et al., 1998; De La Chapelle et al., 1998; Montagnat and Duval, 2004). In this work, we assume that the direct conversion of mechanical energy to heat is the only conversion to heat. This is a reasonable assumption for this work, as to the best of our knowledge there is no proposed mechanism by which strain or surface energy is converted to heat. We leave for future work the consideration of other mechanisms that may alter the energy state of this system (Supplement Text S1). From the processes proposed in Figure 1c, the key mechanisms to model are recrystallization processes and the conversion of mechanical energy to heat through viscous dissipation.

We compute changes in thermal energy using a thermomechanical model, which assumes strain-rate is constant with depth and does not account for softening of ice due to interstitial meltwater (Meyer and Minchew, 2018). We compute changes in strain and surface energy using a steady state grain size model, which parameterizes both migration and rotation recrystallization (Ranganathan et al., 2021). Strain rate is an input to both the grain size and the thermomechanical model, influencing the estimate of Θ. The calculation of Θ depends primarily on 3 other parameters, D, p, and n. The grain-

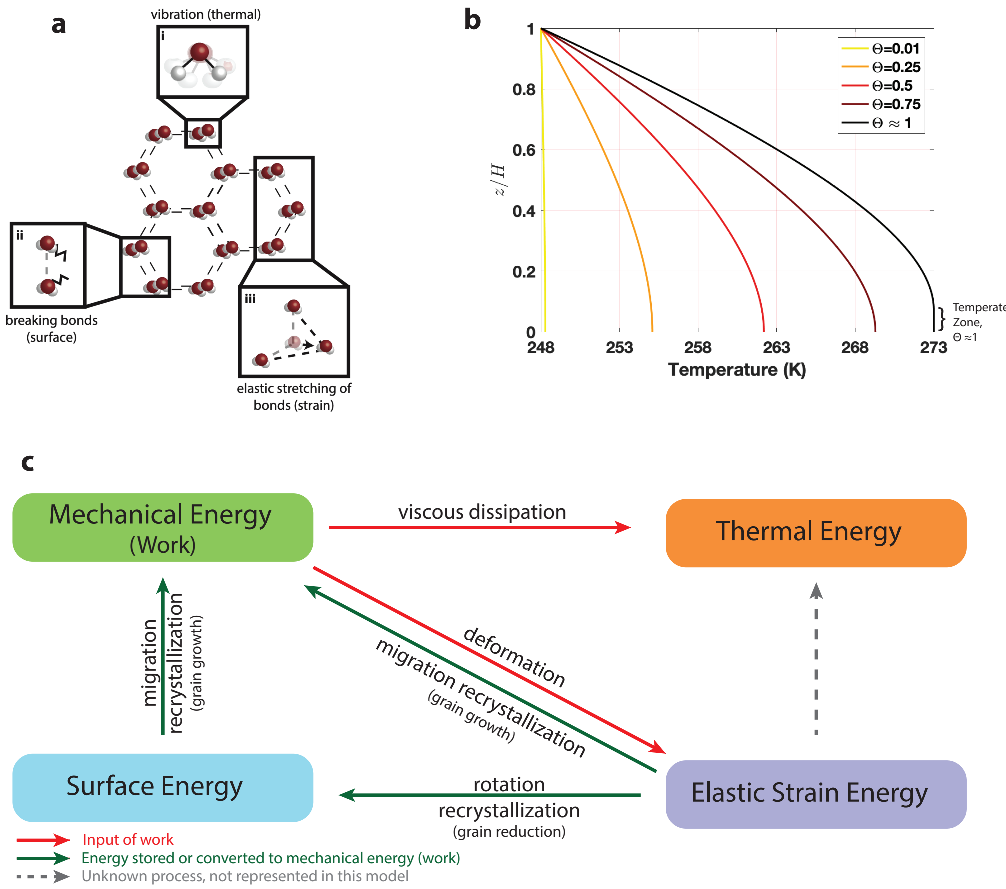

Figure 1. (a) Molecular-scale processes that cause changes in internal energy in glacial ice: (i) vibrational motion of the water molecules in the lattice, which is thermal energy (heat), (ii) breaking of bonds within the lattice, which increases surface energy, (iii) translation of molecules within the lattice relative to their reference position, which stretches or compresses the bonds and increases elastic strain energy. (b) Ice temperature profiles, computed from the model derived by Meyer and Minchew (2018), for varying values of Θ, the fraction of deformational work that is dissipated as heat, with an ice thickness of $H = 1000$ m, a Brinkman number of $\mathrm{Br} = 4$ (which defines the ratio of heat production to conduction), and a Peclet number of $\mathrm{Pe} = 2$ (which in this case defines the ratio of snow accumulation to thermal diffusion). We assume zero heat flux at the bed and a fixed temperature of $-25°$C at the surface, (c) Conservation of energy in glacier shear zones: Mechanical energy is introduced into the system during deformation and is converted into elastic strain energy due to the buildup of dislocations in the crystalline lattice. Strain energy is relieved through recrystallization. Migration recrystallization annihilates dislocations through the outward migration of grain boundaries, which enables further deformation. This mechanism converts elastic strain energy back into mechanical energy and reduces surface energy. Rotation recrystallization reduces strain energy by creating new grain boundaries, which stores the energy in grain boundaries as surface energy. Finally, some mechanical energy is converted into heat and diffused or advected. We assume here that strain energy is not converted into thermal energy, as there is no present mechanism for this to occur (dashed arrow).

growth exponent p partially controls how much grains grow in response to an increase in elastic strain energy, and the characteristic length-scale D describes the length-scale upon which changes in strain energy are considered (approximately the size of a grain). The stress exponent n is the exponent in the constitutive relation that governs ice flow, $\dot{\epsilon} = A\tau^n$, where $\dot{\epsilon}$ is strain-rate, τ is deviatoric stress, and A is the flow-rate parameter, a representation of ice softness.

From estimates of surface, strain, and thermal energy changes, we compute Θ as

$$\Theta(\dot{\epsilon}, n, D, p) = \frac{|\Delta E_{\text{thermal}}|}{|\Delta E_{\text{thermal}}| + |\Delta E_{\text{surface}}| + |\Delta E_{\text{strain}}|} \tag{5}$$

Changes in thermal, surface, and elastic energy depend on Θ, so Equation 5 is a nonlinear equation that is solved here using the Trust-Region-Dogleg algorithm. More detail is presented in Supplement Text S4.

We find changes to surface and strain energy from the steady state grain size model in (Ranganathan et al., 2021) (Supplement Text S3) and changes to thermal energy from the thermomechanical model in (Meyer et al., 2018) (Supplement Text S2):

$$\Delta E_{\text{surface}} = \frac{-c\gamma}{d^2}\Delta d \tag{6a}$$

$$\Delta E_{\text{thermal}} = \rho_i c_p \Delta T \tag{6b}$$

$$\Delta E_{\text{strain}} = -\frac{1}{2}\frac{\tau^2}{\mu}\frac{D^{\frac{p}{2}}}{d^{\frac{p}{2}+1}}\Delta d \tag{6c}$$

Changes to surface energy (Equation 6a) occur from grain size reduction mechanisms and from grain growth during migration recrystallization, where c is a geometric constant based on the shape of grains, γ is grain-boundary energy (a material property), and d is grain size. The expression in Equation 6a was derived by Austin and Evans (2007) and has been subsequently used in rock mechanics and ice studies (Behn et al., 2009, 2020). We estimate changes to thermal energy (Equation 6b) from changes in ice temperature, where ρ_i is the density of ice, c_p is the specific heat capacity of ice, and T is ice temperature. Equation 6b follows directly from the expression for internal energy changes (Equation 2).

Changes to strain energy (Equation 6c) occur due to the reduction in dislocation density during migration recrystallization, where μ is the shear modulus, and D is a characteristic length-scale. The parameterization of strain energy changes presented here is found by assuming that the change of dislocation density is related to the rate of dislocation creation (through deformation) and the rate of dislocation annihilation (through grain-boundary movement and dislocation interactions) and by assuming that the rate of dislocation creation is higher than the rate of dislocation annihilation (Webster, 1966b,a; Karato, 2008). Further, we assume that dislocation creep is the dominant deformation mechanism. While the expression for dislocation density used to derive Equation 6c has been presented in other studies on ice (e.g. Duval et al. (1983); Alley (1992)), other frameworks have been developed to estimate steady-state dislocation density (e.g. Montagnat and Duval (2000); Ng and Jacka (2014)). There are limited observations of the relationship between dislocation density, stress, and strain-rate and further observations could be used to validate which framework is most appropriate for natural conditions of deforming glacier ice. The full derivation of the parameterization for strain energy changes is found in Ranganathan et al. (2021).

The goal of this work is to provide testable predictions for the partitioning of energy in shear margins of glaciers. Here, we estimate the energy partitioning Θ and use this estimate to calculate grain size, ice temperature, and the thickness of temperate zones (zones in which ice has reached its melting point) in West Antarctic shear margins. Grain size is observable by measuring mean grain size from ice cores and borehole samples (e.g. Jackson and Kamb (1997); Gow et al. (1997); Thorsteinsson et al. (1997)) and the existence of temperate zones may be determined by radar. Observations of grain size or ice temperature will provide validation of the concept of energy partitioning and can also be used to illuminate recrystallization processes in natural glacier ice.

3 Estimates of Energy Partitioning in Idealized Setting

We implement this model to estimate Θ in an idealized setting. We consider values of strain rate common in Antarctic ice streams, using the exponent of the flow law $n = 3$, a value which matches laboratory data (Jezek et al., 1985). Supplement Text S5 considers values of $n = 2$ and $n = 4$, both values that correspond with deformation mechanisms (D. L. Goldsby and Kohlstedt, 2001). Past studies have estimated the value of the grain-growth exponent to vary from $p = 2$ to $p > 10$ (Alley et al., 1986b,a; Azuma et al., 2012), with higher values likely more accurate in ice with a significant concentration of bubbles, such as glacial ice (Azuma et al., 2012). The value of the characteristic length-scale D likely falls between 10 and 100 mm due to the average size of crystals in ice. We treat both D and p as constrained but uncertain parameters and determine Θ for a D-p parameter space.

Figure 2 (top row) shows Θ for expected values of D and p and for 3 different glaciologically-relevant strain rates. Supplement Text S5 presents full temperature and grain size profiles with depth for these three strain rates and for varying Θ values. In general, we find that surface energy changes are ~ 3 orders of magnitude lower than both strain energy and thermal energy changes. For all strain rates, there are approximately two distinct solutions for different p and D values, due to E_{surface} being negligible in most cases (Supplement Text S4). There is a narrow boundary between the two that contains values between the two solutions. This boundary widens for lower values of n. However, this boundary is narrow enough for most physically reasonable values of n that the probability of the true values of D and p falling in that boundary are small enough to warrant neglecting it for our purposes. This quasi-binary behavior suggests that for any given strain rate, there are only two likely estimates of Θ.

In glaciers, the strain rates in shear margins are generally $\sim 10^{-9}$ s^{-1}, approaching 10^{-8} s^{-1} only in the shear margins of glaciers that deform extremely quickly, such as Pine Island Glacier, West Antarctica (Gardner et al., 2018). Thus, we take the middle panel of the top row of Figure 2 ($\dot{\epsilon} = 10^{-9}$ s^{-1}) to be the case that most closely resembles the conditions in Antarctic ice streams, in which the two solutions are $\Theta \approx 1$ (Regime A) and $\Theta \approx \frac{1}{2}$ (Regime B).

We now consider these two regimes in more detail. (Figure 2; bottom row). As shown in the derivation of the thermomechanical model used here (Meyer and Minchew, 2018), ice temperature (and the strain rate at which temperate ice forms) can be written as a function of two non-dimensional numbers: the Brinkman number, which describes the ratio of the rate of heat production through viscous dissipation to thermal conduction, and the Peclet number, which describes the ratio of advection of cold ice driven by snow accumulation to thermal diffusion. The Brinkman and Peclet numbers are described in Supplement Text S2. Figure 2 presents estimates of Θ for typical values of the Brinkman and Peclet numbers found in the modern Antarctic Ice Sheet (Meyer and Minchew, 2018).

In Regime A (Figure 2A), $\Theta = 1$ for all physically realistic values of the Brinkman number and the Peclet number. In Regime B (Figure 2B), Θ varies based on strain rate from $\Theta = \frac{1}{2}$ at higher strain rates (higher values of the Brinkman number) to $\Theta = 1$ at lower strain rates (lower values of the Brinkman number). Θ is lower at high strain

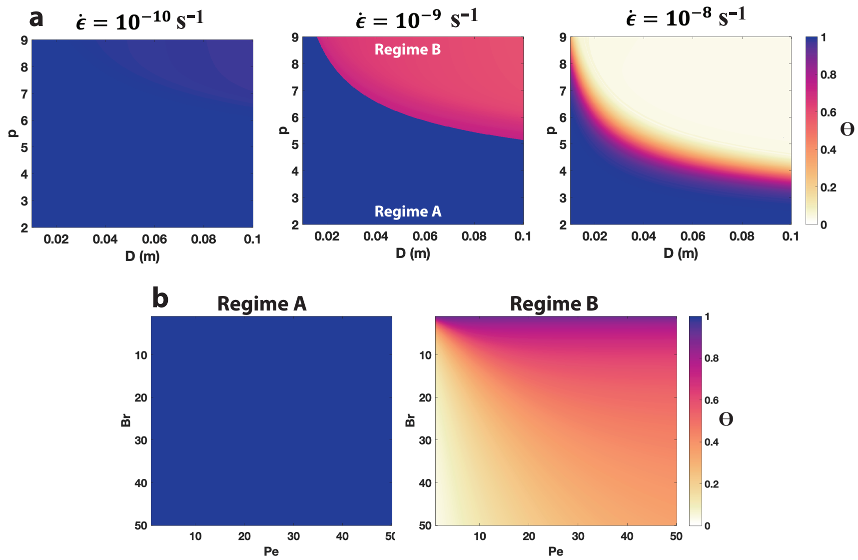

Figure 2. (a) Estimated values of Θ for varying characteristic length scale for migration recrystallization, D, grain growth exponent, p, and lateral shear strain rate $\dot{\epsilon}$ for flow law exponent $n = 3$. For each case, there are two clear regimes for varying D and p, which we label Regime A and Regime B (middle panel). (b) Estimated values of Θ for varying Brinkman number (ratio of the rate of heat production to thermal conduction) and Peclet number (ratio of accumulation to thermal diffusion) in (1) Regime A, in which $\Theta = 1$ for all combinations of the Brinkman and Peclet numbers, and (2) Regime B, in which $\Theta < 1$ for almost the entire domain, and Θ increases for decreasing Brinkman number.

rates due to the increase in elastic strain energy with rapid deformation, resulting in a lower fraction of work dissipated as heat and an increased fraction of work driving recrystallization.

Comparisons of the model with data suggests Regime B may best apply to natural deforming glacier ice. Ranganathan et al. (2021) compared outputs of this steady state grain size model to ice core data of grain sizes with depth to constrain values of p and D. The most likely values of p fall between $p = 6$ and $p = 9$ and the most likely values of D fall between $D = 50$ mm and $D = 100$ mm. This may imply that $\Theta \approx \frac{1}{2}$ for $\dot{\epsilon} = 10^{-9}$ s^{-1}. However, there is enough uncertainty in both D and p that both solutions can be thought of as valid barring further data collected on either average grain size or grain growth kinetics in natural deforming ice. These results suggests that when we consider the energy budget of ice, recrystallization and grain-scale processes in rapidly-deforming regions may play a significant role.

4 Estimates of Energy Partitioning in Shear Margins of Antarctic Ice Streams

The method of finding Θ presented here is particularly useful because it can be applied to Antarctic ice streams using observable data. The thermomechanical model finds ice temperature from surface strain rates and ice thickness (Meyer and Minchew, 2018), both observable quantities, and the steady state grain-size model predicts grain sizes from ice temperature and surface strain rates (Ranganathan et al., 2021). Here, we apply this method to find this energy partitioning Θ in Antarctic glacier shear margins. We consider the case of Pine Island Glacier in the Amundsen Sea Embayment because Pine Is-

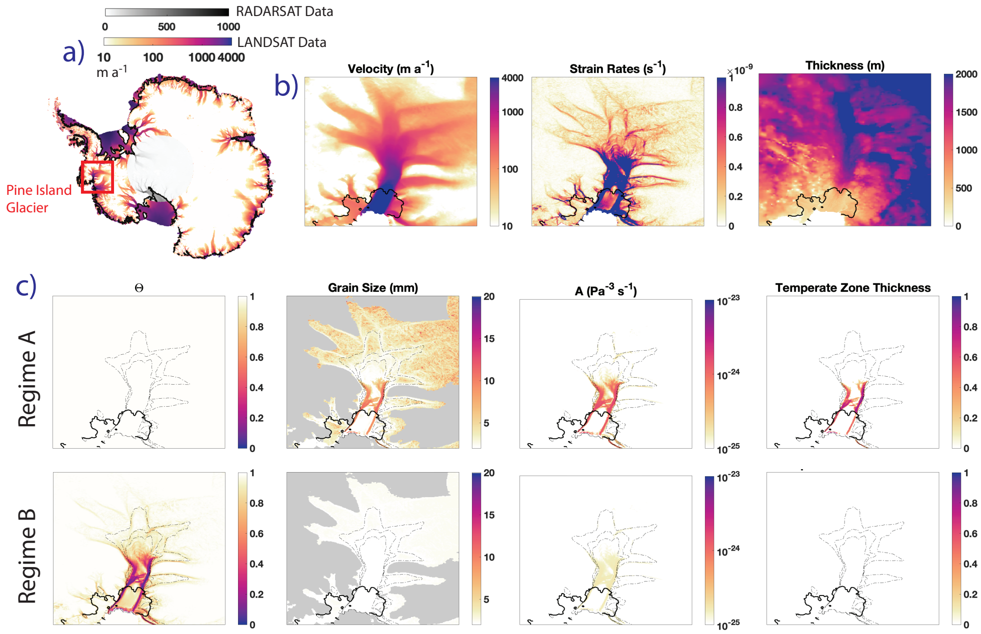

Figure 3. Strain rates computed from surface velocity fields derived from Landsat 7 and 8 (Gardner et al., 2018) (area south of −83.5 degrees filled by RADARSAT, shown in greyscale (Mouginot et al., 2012)) and thickness computed from REMA surface elevation (Howat et al., 2019) and BedMachine bed topography (Morlighem et al., 2020) in the first row. Second and third rows show estimated values of Θ, the depth-averaged flow-rate parameter, steady state depth-averaged grain size, and the thickness of temperate zones as a fraction of ice thickness in Pine Island Glacier for both regimes (Regime A: $D = 0.05$ mm, $p = 2$, Regime B: $D = 0.05$ mm, $p = 9$).

land Glacier deforms quite rapidly, with surface velocities of up to ~ 4000 m a^{-1} and strain rates in the margins of $\sim 10^{-8}$ s^{-1}.

To compute ice temperature, steady state grain size, and Θ, we use data of surface strain rates computed from surface velocity observations (Gardner et al., 2018) and ice thickness, found from REMA surface elevation and BedMachine basal topography (Howat et al., 2019; Morlighem et al., 2020). We estimate Θ for both regimes, as described in the previous section, and compare the effect of Θ on grain size, the flow-rate parameter, and the thickness of the temperate zone. The flow-rate parameter, a measure of ice softness as a function of temperature, crystallographic fabric, porosity, and liquid water content, is computed by an Arrhenius relation $A = A_0 \exp\left[\frac{-Q_c}{RT}\right]$, where Q_c is the activation energy for creep, R is the ideal gas constant, and A_0 is a prefactor (Cuffey and Paterson, 2010). However, factors like grain-size and fabric may affect the flow-rate parameter in ways not currently represented in ice-flow models, as discussed below. The thickness of the temperate zone measures the thickness of the ice at its melting point. Results for other glaciers are shown in Supplement Text S6.

Regime A, represented by $D = 0.05$ m and $p = 2$, estimates $\Theta = 1$ over the domain, suggesting that all deformational work is dissipated as heat. In this regime, ice temperature is high due to the significance of heating. Migration recrystallization responds strongly to temperature, since high temperature is required for rapid grain boundary migration and thus an increase in grain size. Therefore, in this regime, grain sizes are large

($\sim$ 15 mm). In a regime where $\Theta = 1$, the rate of shear heating is high, and therefore the flow-rate parameter is elevated between 1-2 orders of magnitude from the centerline. Deformational heating also produces a very significant temperate zone, extending to $\sim$ 80% of the local ice thickness.

In Regime B, found by setting $D = 0.05$ and $p = 9$ (with the higher value of p most applicable to ice with bubbles), we estimate $\Theta < 1$ in the shear margins. High strain rates and thus high temperatures and large changes in elastic strain energy drive dynamic recrystallization, resulting in a partitioning of deformational work primarily into thermal energy and elastic strain energy. In the fastest-deforming regions, Θ reaches as low as $\Theta \approx 0.1$. This suggests that a significant portion of the work is being stored by recrystallization mechanisms rather than being dissipated as heat. Since ice temperature remains low, migration recrystallization is not significantly activated and grain sizes remain small ($\sim 1 - 2$ mm). In Regime B, the estimate of the flow-rate parameter is elevated only by about half an order of magnitude, rather than 1-2 orders of magnitude as shown in Regime A, suggesting more viscous ice in Regime B than in Regime A. This regime produces a minimal temperate zone, small enough to be neglected by ice flow models, due to this partitioning of energy and thus diminished heating. This suggests that previous work may have overestimated the presence of temperate ice in active shear margins.

Constraining the value of Θ is therefore important when modeling ice dynamics, as the value of this energy partitioning parameter affects ice temperature and ice softness significantly. The flow-rate parameter has a first-order effect on the rheology of ice, through the flow law, and using higher values of the flow-rate parameter are likely to produce faster flows and thus faster mass loss in ice flow models. Further, as explored in Ranganathan et al. (2021), grain size also affects the value of the flow-law exponent n, which provides a significant control on flow speed. Large grain sizes allow for flow through dislocation creep ($n = 4$), a mechanism of creep in which ice flows through line defects called dislocations. Small grain sizes, on the other hand, allow for grain-size-dependent creep mechanisms such as grain boundary sliding ($n = 2$) (D. Goldsby and Kohlstedt, 1997; D. L. Goldsby and Kohlstedt, 1997, 2001). The feedbacks between Θ, grain size, and the rate of deformation as partially dictated by the stress exponent n suggests that integrating the effects of dynamic recrystallization and considering the partitioning of deformational energy changes between thermal energies, strain energies, and surface energies in large ice flow models is necessary to gain accurate projections of glacier behavior.

Further, this model allows for an examination of the important parameters affecting ice rheology. Here, the grain-growth exponent p has a leading order effect on ice rheology in shear margins. The value of this grain-growth exponent partially controls which regime ($\Theta = 1$ or $\Theta < 1$ in shear margins) is applicable to naturally-deforming glaciers and thus has a significant effect on ice rheology in fast-flowing glaciers. The grain-growth exponent p is not well constrained, and values from laboratory experiments have found exponents ranging from $2-20$, based on variations in bubble concentration, impurities, and ice microstructure (Alley et al., 1986b,a; Azuma et al., 2012). More accurate constraints on this grain-growth exponent are then likely to improve our ability to project changes in ice rheology.

This model does not take into account the effect of fabric development due to the lack of a clear connection between fabric development and changes in surface and strain energy. The inclusion of fabric into this formulation of the energy balance will likely enhance the results shown here, since deformational energy would then be a partition between thermal energy, surface and strain energy from changes in grain size, and surface and strain energy from changes in grain orientation. We reserve exploration of the effects of fabric for future work.

Though we do not explicitly account for fabric in this model, this work does further support the need for a parameterization of the effect of fabric development on ice softness. With the solely-temperature-dependent flow rate parameter, the results here suggest that the ice in Regime A is softer than the ice in Regime B due to the rate of heating in Regime A being higher than that in Regime B. However, including fabric may affect the ice softness (flow-rate parameter) results shown in Regimes A and B. Recrystallization mechanisms produce distinct fabrics, and therefore the fabrics in the two regimes may be distinct due to differences in the prevalence of recrystallization mechanisms (Wenk et al., 1997; Faria, 2006a; Faria et al., 2006; Faria, 2006b; Journaux et al., 2019). Previous estimates have suggested that fabric development likely increases the flow rate parameter, and thus strain-rates, by approximately an order of magnitude (Minchew et al., 2018). This illustrates the need for a more complete formulation of the flow rate parameter that takes into account the contributions from fabric softening, as well as a more complete flow law that accounts for anisotropy. We also reserve an exploration of the effect of fabric on ice rheology in this context for future work.

Finally, the thermomechanical model used here does not consider the effect of lateral advection of cold, isotropic ice into the glacier shear margins during deformation (Suckale et al., 2014; Meyer and Minchew, 2018). This advection is likely to dampen some of the heating effects by introducing cold ice into the shear margin (Haseloff et al., 2019; Hunter et al., 2021). However, the effects would not likely impact the estimates here, since the advective timescale (approximately the width of the shear margin divided by the rate of flow into the shear margin) would be much longer than the time to steady-state (Ranganathan et al., 2021). The combined effects of grain size evolution and lateral advection can be explored in a framework similar to that of Hunter et al. (2021).

5 Conclusions

Constraining the energy budget in glaciers is a critical part of understanding glacial dynamics. On a molecular-scale, we know that the changes in energy arise from a combination of surface energy, strain energy, and thermal energy if the ice is below the melting point. However, on a macro-scale when considering ice dynamics, we generally neglect elastic strain energy and surface energy, prioritizing the impact of changes in thermal energy to glacier flow. Here, we show that changes in strain and surface energy may be an important factor in the energy budget of glacier shear margins, and thus models of ice flow should take into account changes in non-thermal energy through parameterizations of dynamic recrystallization processes.

The validity of our model and the question of which regime is most applicable to natural glaciers can be tested against observations. The overall difference in grain size between the two regimes is large enough to be observable, with one regime (Regime A) having high enough heating rates to activate migration recrystallization and thus produce large grain sizes, while the other (Regime B) having low heating rates and therefore maintaining small grain sizes. There are a few observations of grain sizes in shear margins, including in shallow boreholes in West Antarctica (Jackson and Kamb, 1997) and in an Alaskan glacier (Gerbi et al., 2021), and a few observations of grain size in temperate glaciers (Tison and Hubbard, 2000). These observations show relatively large grain sizes, though observations of temperate glaciers and glaciers outside of Antarctica may not be applicable to shear margin conditions in West Antarctica and shallow boreholes may not be sufficient to capture the variation in grain size spatially and with depth. More observations of grain sizes, both broadly and in shear margins, may provide sufficient evidence to suggest which regime is applicable to Antarctic glaciers, which would then enable estimates of Θ across the ice sheet.

The incorporation of non-thermal energy changes into ice flow models can be readily done in the existing framework of the models. Adding the parameter Θ to the work term in the energy balance already used in ice flow models would be a simple way of producing more accurate estimates of ice temperature and ice rheology and would not require any reworking of current ice flow models. Future work will involve incorporating the effects of fabric and lateral advection into this framework, which will improve the accuracy of Θ estimates and provide a more complete picture of the energy balance within glaciers. Through the inclusion of dynamic recrystallization in models of glacial dynamics in zones of high shear, we provide a step towards understanding the effect of dynamic recrystallization and grain-scale processes on ice flow, as well as understanding the energetics within rapidly deforming regions of glaciers.

Acknowledgments

The authors gratefully acknowledge conversations and feedback from Alan Rempel, Ed Bueler, David Prior, and Terry Yu. M.I.R. was funded through the Martin Fellowship, the Sven Treitel Fellowship, and NSFGEO-NERC award 1853918. B.M.M. was funded through award 1853918, NSF-NERC award 1739031, and NEC Corporation Fund for Research in Computers and Communications. No new data were produced for this study, and data used in this study are publicly available through their respective publications, cited here. The codes for the grain size and ice temperature models are found at 10.5281/zenodo.5121903.

References

Alley, R. [1992, jan]. Flow-law hypotheses for ice-sheet modeling. *Journal of Glaciology*, *38*(129), 245–256. https://www.cambridge.org/core/product/identifier/S0022143000003658/type/journal{_}article doi: 10.3189/S0022143000003658

Alley, R., Perepezko, J., and Bentley, C. [1986a, jan]. Grain Growth in Polar Ice: II. Application. *Journal of Glaciology*, *32*(112), 425–433. https://www.cambridge.org/core/product/identifier/S0022143000012132/type/journal{_}article doi: 10.3189/S0022143000012132

Alley, R., Perepezko, J., and Bentley, C. [1986b]. Grain Growth in Polar Ice: I. Theory. *Journal of Glaciology*, *32*(112), 425–433. doi: 10.3189/s0022143000012132

Austin, N. J., and Evans, B. [2007]. Paleowattmeters: A scaling relation for dynamically recrystallized grain size. *Geology*, *35*(4), 343. https://pubs.geoscienceworld.org/geology/article/35/4/343-346/129818 doi: 10.1130/G23244A.1

Azuma, N., Miyakoshi, T., Yokoyama, S., and Takata, M. [2012, sep]. Impeding effect of air bubbles on normal grain growth of ice. *Journal of Structural Geology*, *42*, 184–193. http://dx.doi.org/10.1016/j.jsg.2012.05.005https://linkinghub.elsevier.com/retrieve/pii/S019181411200123X doi: 10.1016/j.jsg.2012.05.005

Behn, M. D., Goldsby, D. L., and Hirth, G. [2020]. The role of grain-size evolution on the rheology of ice: Implications for reconciling laboratory creep data and the Glen flow law. *The Cryosphere Discussions*(November), 1–31. https://tc.copernicus.org/preprints/tc-2020-295/ doi: 10.5194/tc-2020-295

Behn, M. D., Hirth, G., and Elsenbeck II, J. R. [2009, may]. Implications of grain size evolution on the seismic structure of the oceanic upper mantle. *Earth and Planetary Science Letters*, *282*(1-4), 178–189. http://dx.doi.org/10.1016/j.epsl.2009.03.014https://linkinghub.elsevier.com/retrieve/pii/S0012821X09001575 doi: 10.1016/j.epsl.2009.03.014

Cuffey, K., and Paterson, W. [2010]. *The Physics of Glaciers* (Fourth ed.). Elsevier.

De Bresser, J. H. P., Peach, C. J., Reijs, J. P. J., and Spiers, C. J. [1998, sep]. On dynamic recrystallization during solid state flow: Effects of stress and temperature. *Geophysical Research Letters*, *25*(18), 3457–3460. http://doi.wiley.com/10.1029/98GL02690 doi: 10.1029/98GL02690

De La Chapelle, S., Castelnau, O., Lipenkov, V., and Duval, P. [1998, mar]. Dynamic recrystallization and texture development in ice as revealed by the study of deep ice cores in Antarctica and Greenland. *Journal of Geophysical Research: Solid Earth*, *103*(B3), 5091–5105. http://doi.wiley.com/10.1029/97JB02621 doi: 10.1029/97JB02621

Derby, B. [1992, dec]. Dynamic recrystallisation: The steady state grain size. *Scripta Metallurgica et Materialia*, *27*(11), 1581–1585. https://linkinghub.elsevier.com/retrieve/pii/0956716X92901488 doi: 10.1016/0956-716X(92)90148-8

Derby, B., and Ashby, M. [1987, jun]. On dynamic recrystallisation. *Scripta Metallurgica*, *21*(6), 879–884. https://linkinghub.elsevier.com/retrieve/pii/0036974887903413 doi: 10.1016/0036-9748(87)90341-3

Duval, P., Ashby, M. F., and Anderman, I. [1983]. Rate-controlling processes in the creep of polycrystalline ice. *Journal of Physical Chemistry*, *87*(21), 4066–4074. doi: 10.1021/j100244a014

Duval, P., and Castelnau, O. [1995]. Dynamic recrystallization of ice in polar ice sheets. *Journal de Physique IV*, *5*(C3), 197–205. http://www.scopus.com/inward/record.url?eid=2-s2.0-33750590172{\&}partnerID=MN8TOARS doi: 10.1051/jp4

Echelmeyer, K. A., Harrison, W. D., Larsen, C., and Mitchell, J. E. [1994, jan]. The role of the margins in the dynamics of an active ice stream. *Journal of Glaciology*, *40*(136), 527–538. https://www.cambridge.org/core/product/identifier/S0022143000012417/type/journal{_}article doi: 10.1017/S0022143000012417

Faria, S. H. [2006a]. Creep and recrystallization of large polycrystalline masses. I. General continuum theory. *Proceedings of the Royal Society A: Mathematical, Physical and Engineering Sciences*, *462*(2069), 1493–1514. doi: 10.1098/rspa.2005.1610

Faria, S. H. [2006b]. Creep and recrystallization of large polycrystalline masses. III. Continuum theory of ice sheets. *Proceedings of the Royal Society A: Mathematical, Physical and Engineering Sciences*, *462*(2073), 2797–2816. doi: 10.1098/rspa.2006.1698

Faria, S. H., Kremer, G. M., and Hutter, K. [2006]. Creep and recrystallization of large polycrystalline masses. II. Constitutive theory for crystalline media with transversely isotropic grains. *Proceedings of the Royal Society A: Mathematical, Physical and Engineering Sciences*, *462*(2070), 1699–1720. doi: 10.1098/rspa.2005.1635

Gardner, A. S., Moholdt, G., Scambos, T., Fahnstock, M., Ligtenberg, S., van den Broeke, M., and Nilsson, J. [2018, feb]. Increased West Antarctic and unchanged East Antarctic ice discharge over the last 7 years. *The Cryosphere*, *12*(2), 521–547. https://tc.copernicus.org/articles/12/521/2018/ doi: 10.5194/tc-12-521-2018

Gerbi, C., Mills, S., Clavette, R., Campbell, S., Bernsen, S., Clemens-Sewall, D., ... Hruby, K. [2021, jun]. Microstructures in a shear margin: Jarvis Glacier, Alaska. *Journal of Glaciology*, 1–14. https://www.cambridge.org/core/product/identifier/S0022143021000629/type/journal{_}article doi: 10.1017/jog.2021.62

Goldsby, D., and Kohlstedt, D. [1997, nov]. Grain boundary sliding in fine-grained Ice I. *Scripta Materialia*, *37*(9), 1399–1406. https://linkinghub.elsevier.com/retrieve/pii/S1359646297002467 doi: 10.1016/S1359-6462(97)00246-7

Goldsby, D. L., and Kohlstedt, D. L. [1997]. Flow of ice by Dislocation, Grain Boundary Sliding, and Diffusion Processes. *Lunar and Planetary Science*.

Goldsby, D. L., and Kohlstedt, D. L. [2001, jun]. Superplastic deformation of ice: Experimental observations. *Journal of Geophysical Research: Solid Earth*, *106*(B6), 11017–11030. http://doi.wiley.com/10.1029/2000JB900336 doi: 10.1029/2000JB900336

Gow, A. J., Meese, D. A., Alley, R. B., Fitzpatrick, J. J., Anandakrishnan, S., Woods, G. A., and Elder, B. C. [1997, nov]. Physical and structural properties of the Greenland Ice Sheet Project 2 ice core: A review. *Journal of Geophysical Re-*

search: Oceans, *102*(C12), 26559–26575. http://doi.wiley.com/10.1029/97JC00165 doi: 10.1029/97JC00165

Haseloff, M., Hewitt, I. J., and Katz, R. F. [2019, nov]. Englacial Pore Water Localizes Shear in Temperate Ice Stream Margins. *Journal of Geophysical Research: Earth Surface*, *124*(11), 2521–2541. https://onlinelibrary.wiley.com/doi/abs/10.1029/2019JF005399 doi: 10.1029/2019JF005399

Hindmarsh, R. [2004, mar]. Thermoviscous stability of ice-sheet flows. *Journal of Fluid Mechanics*, *502*, 17–40. http://www.journals.cambridge.org/abstract{_}S0022112003007390 doi: 10.1017/S0022112003007390

Hodowany, J., Ravichandran, G., Rosakis, A. J., and Rosakis, P. [2000]. Partition of plastic work into heat and stored energy in metals. *Experimental Mechanics*, *40*(2), 113–123. doi: 10.1007/BF02325036

Howat, I. M., Porter, C., Smith, B. E., Noh, M.-J., and Morin, P. [2019, feb]. The Reference Elevation Model of Antarctica. *The Cryosphere*, *13*(2), 665–674. https://tc.copernicus.org/articles/13/665/2019/ doi: 10.5194/tc-13-665-2019

Hunter, P., Meyer, C., Minchew, B., Haseloff, M., and Rempel, A. [2021]. Thermal controls on ice stream shear margins. *Journal of Glaciology*, 1–15. doi: 10.1017/jog.2020.118

Jackson, M., and Kamb, B. [1997, jan]. The marginal shear stress of Ice Stream B, West Antarctica. *Journal of Glaciology*, *43*(145), 415–426. https://www.cambridge.org/core/product/identifier/S0022143000035000/type/journal{_}article doi: 10.3189/S0022143000035000

Jacobson, H. P., and Raymond, C. F. [1998, jun]. Thermal effects on the location of ice stream margins. *Journal of Geophysical Research: Solid Earth*, *103*(B6), 12111–12122. http://doi.wiley.com/10.1029/98JB00574 doi: 10.1029/98JB00574

Jezek, K., Alley, R., and Thomas. [1985, mar]. Rheology of Glacier Ice. *Science*, *227*(4692), 1335–1337. https://www.sciencemag.org/lookup/doi/10.1126/science.227.4692.1335 doi: 10.1126/science.227.4692.1335

Journaux, B., Chauve, T., Montagnat, M., Tommasi, A., Barou, F., Mainprice, D., and Gest, L. [2019]. Recrystallization processes, microstructure and crystallographic preferred orientation evolution in polycrystalline ice during high-temperature simple shear. *Cryosphere*, *13*(5), 1495–1511. doi: 10.5194/tc-13-1495-2019

Karato, S.-i. [2008]. *Deformation of Earth Materials: An Introduction to the Rheology of Solid Earth.* Cambridge University Press.

Mason, J. J., Rosakis, A. J., and Ravichandran, G. [1994]. On the strain and strain rate dependence of the fraction of plastic work converted to heat: an experimental study using high speed infrared detectors and the Kolsky bar. *Mechanics of Materials*, *17*(2-3), 135–145. doi: 10.1016/0167-6636(94)90054-X

Meyer, C. R., Fernandes, M. C., Creyts, T. T., and Rice, J. R. [2016, aug]. Effects of ice deformation on Röthlisberger channels and implications for transitions in subglacial hydrology. *Journal of Glaciology*, *62*(234), 750–762. https://www.cambridge.org/core/product/identifier/S0022143016000654/type/journal{_}article doi: 10.1017/jog.2016.65

Meyer, C. R., and Minchew, B. M. [2018, sep]. Temperate ice in the shear margins of the Antarctic Ice Sheet: Controlling processes and preliminary locations. *Earth and Planetary Science Letters*, *498*, 17–26. https://doi.org/10.1016/j.epsl.2018.06.028https://linkinghub.elsevier.com/retrieve/pii/S0012821X18303790 doi: 10.1016/j.epsl.2018.06.028

Meyer, C. R., Yehya, A., Minchew, B., and Rice, J. R. [2018, aug]. A Model for the Downstream Evolution of Temperate Ice and Subglacial Hydrology Along Ice Stream Shear Margins. *Journal of Geophysical Research: Earth Surface*, *123*(8), 1682–1698. https://onlinelibrary.wiley.com/doi/abs/10.1029/2018JF004669 doi: 10.1029/2018JF004669

Minchew, B. M., Meyer, C. R., Robel, A. A., Gudmundsson, G. H., and Simons, M. [2018, aug]. Processes controlling the downstream evolution of ice rheology in glacier shear margins: case study on Rutford Ice Stream, West Antarctica. *Journal of Glaciology*, *64*(246), 583–594. https://www.cambridge.org/core/product/identifier/S0022143018000473/type/journal{_}article doi: 10.1017/jog.2018.47

Montagnat, M., and Duval, P. [2000, nov]. Rate controlling processes in the creep of polar ice, influence of grain boundary migration associated with recrystallization. *Earth and Planetary Science Letters*, *183*(1-2), 179–186. https://linkinghub.elsevier.com/retrieve/pii/S0012821X00002624 doi: 10.1016/S0012-821X(00)00262-4

Montagnat, M., and Duval, P. [2004]. Dislocations in ice and deformation mechanisms: From single crystals to polar ice. *Defect and Diffusion Forum*, *229*(January 2017), 43–54. doi: 10.4028/www.scientific.net/ddf.229.43

Morlighem, M., Rignot, E., Binder, T., Blankenship, D., Drews, R., Eagles, G., … Young, D. A. [2020]. Deep glacial troughs and stabilizing ridges unveiled beneath the margins of the Antarctic ice sheet. *Nature Geoscience*, *13*(2), 132–137. http://dx.doi.org/10.1038/s41561-019-0510-8 doi: 10.1038/s41561-019-0510-8

Mouginot, J., Scheuch, B., and Rignot, E. [2012]. Mapping of ice motion in antarctica using synthetic-aperture radar data. *Remote Sensing*, *4*(9), 2753–2767. doi: 10.3390/rs4092753

Ng, F., and Jacka, T. [2014, jul]. A model of crystal-size evolution in polar ice masses. *Journal of Glaciology*, *60*(221), 463–477. https://www.cambridge.org/core/product/identifier/S0022143000205947/type/journal{_}article doi: 10.3189/2014JoG13J173

Perol, T., and Rice, J. R. [2015, may]. Shear heating and weakening of the margins of West Antarctic ice streams. *Geophysical Research Letters*, *42*(9), 3406–3413. http://doi.wiley.com/10.1002/2015GL063638 doi: 10.1002/2015GL063638

Ranganathan, M., Minchew, B., Meyer, C., and Pec, M. [2021]. *Recrystallization of ice enhances the creep and vulnerability to fracture of ice shelves.* doi: 10.31223/X5W31W

Rignot, E. [2004]. Accelerated ice discharge from the Antarctic Peninsula following the collapse of Larsen B ice shelf. *Geophysical Research Letters*, *31*(18), L18401. http://doi.wiley.com/10.1029/2004GL020697 doi: 10.1029/2004GL020697

Rollett, A. D., and Kocks, U. [1993]. A Review of the Stages of Work Hardening. *Solid State Phenomena*, *35-36*(January), 1–18. doi: 10.4028/www.scientific.net/ssp.35-36.1

Rosakis, P., Rosakis, A. J., Ravichandran, G., and Hodowany, J. [2000]. Thermodynamic internal variable model for the partition of plastic work into heat and stored energy in metals. *Journal of the Mechanics and Physics of Solids*, *48*(3), 581–607. doi: 10.1016/S0022-5096(99)00048-4

Schoof, C. [2004, sep]. On the mechanics of ice-stream shear margins. *Journal of Glaciology*, *50*(169), 208–218. http://www.ingentaconnect.com/content/igsoc/jog/2004/00000050/00000169/art00005https://www.cambridge.org/core/product/identifier/S0022143000214275/type/journal{_}article doi: 10.3189/172756504781830024

Schoof, C. [2012, dec]. Thermally driven migration of ice-stream shear margins. *Journal of Fluid Mechanics*, *712*, 552–578. https://www.cambridge.org/core/product/identifier/S0022112012004387/type/journal{_}article doi: 10.1017/jfm.2012.438

Suckale, J., Platt, J. D., Perol, T., and Rice, J. R. [2014, may]. Deformation-induced melting in the margins of the West Antarctic ice streams. *Journal of Geophysical Research: Earth Surface*, *119*(5), 1004–1025. http://doi.wiley.com/10.1002/2013JF003008 doi: 10.1002/2013JF003008

Thorsteinsson, T., Kipfstuhl, J., and Miller, H. [1997]. Textures and fabrics in the

GRIP ice core. *Journal of Geophysical Research: Oceans*, *102*(C12), 26583–26599. doi: 10.1029/97JC00161

Tison, J. L., and Hubbard, B. [2000]. Ice crystallographic evolution at a temperate glacier: Glacier de Tsanfleuron, Switzerland. *Geological Society Special Publication*, *176*, 23–38. doi: 10.1144/GSL.SP.2000.176.01.03

Webster, G. A. [1966a]. In support of a model of creep based on dislocation dynamics. *Philosophical Magazine*, *14*(132), 1303–1307. doi: 10.1080/14786436608224296

Webster, G. A. [1966b]. A widely applicable dislocation model of creep. *Philosophical Magazine*, *14*(130), 775–783. doi: 10.1080/14786436608211971

Wenk, H. R., Canova, G., Bréchet, Y., and Flandin, L. [1997]. A deformation-based model for recrystallization of anisotropic materials. *Acta Materialia*, *45*(8), 3283–3296. doi: 10.1016/S1359-6454(96)00409-0

Wilson, C. J., and Zhang, Y. [1996]. Development of microstructure in the high-temperature deformation of ice. *Annals of Glaciology*, *23*, 293–302. doi: 10.3189/s0260305500013562

Wingham, D. J., Wallis, D. W., and Shepherd, A. [2009]. Spatial and temporal evolution of Pine Island Glacier thinning, 1995-2006. *Geophysical Research Letters*, *36*(17), 5–9. doi: 10.1029/2009GL039126

Supporting Information for "Deformational-energy partitioning in glacier shear zones"

Meghana Ranganathan[1], Brent Minchew[1], Colin R. Meyer[2], Matěj Peč[1]

[1]Department of Earth, Atmospheric and Planetary Sciences, Massachusetts Institute of Technology, Cambridge, MA, USA

[2]Thayer School of Engineering, Dartmouth College, Hanover, NtH, USA

Contents of this file

1. Conservation of Energy

The first law of thermodynamics is

$$\dot{U} = \dot{Q} + \dot{W} \tag{1}$$

where $\dot{U}$ is the rate of change of internal energy, $\dot{Q}$ is the rate of change of energy supplied through heat, and $\dot{W}$ is the rate of work done on volume Ω by the surrounding material. The rate of change of internal energy can be found by:

$$\dot{U} = \frac{D}{Dt}\int_{\Omega}(\rho c_p T + \frac{1}{2}\rho u_i u_i + E_{\text{non-thermal}})dV \tag{2}$$

where $\frac{D}{Dt}$ is the material derivative, c_p is the specific heat capacity of ice, T is ice temperature, u_i is the velocity of the ice, $\rho c_p T$ is the thermal energy, and $\frac{1}{2}\rho u_i u_i$ is the kinetic energy and where repeating indices indicate summation. As defined in Ranganathan et al. (2021), $E_{\text{non-thermal}}$ can be approximated by the change in energy due to recrystallization, assuming recrystallization is the dominant mechanism altering the strain and surface energy state of the ice, such that $\dot{E}_{\text{non-thermal}} = \dot{E}_{\text{surface}} - \dot{E}_{\text{strain}}$, in which $\dot{E}_{\text{surface}}$ is the rate of change of surface energy during rotation recrystallization and $\dot{E}_{\text{strain}}$ is the rate of change of strain energy during migration recrystallization, with the overdot denoting a time derivative. Both E_{surface} and E_{strain} can be found by considering the grain size and dislocation density within the grains, such that

$$\dot{E}_{\text{surface}} - \dot{E}_{\text{strain}} = \frac{c\gamma}{d} - \frac{1}{2}\left(\frac{D}{d}\right)^{\frac{p}{2}}\frac{\tau_s^2}{\mu} \tag{3}$$

where p is the grain-growth exponent, D is the characteristic length-scale, τ_s is the shear stress, and d is the grain size. The full derivation is found in Ranganathan et al. (2021).

The rate of heat transfer by conduction can be found from Fourier's Law as

$$\dot{Q} = -\int_{\partial\Omega} KT_{,j}(-n_j)ds \tag{4}$$

where K is the thermal conductivity. The rate of work done by the surrounding material is

$$\dot{W} = -\int_{\partial\Omega} \tau_{ij}u_i(-n_j)ds + \int_{\Omega} \rho g_i u_i dV \tag{5}$$

In this study, we assume incompressibility and we neglect kinetic energy, as we are in a low Reynolds number regime and therefore kinetic energy is likely to be negligible. Thus, internal energy U is approximately equivalent to enthalpy H such that Equation 2 can be written in terms of enthalpy as

$$H = \rho c_p T + \frac{c\gamma}{d} - \frac{1}{2}\left(\frac{D}{d}\right)^{\frac{p}{2}}\frac{\tau_s^2}{\mu} + H_0 \tag{6}$$

where H_0 is a constant offset. From the first law of thermodynamics, writing in terms of enthalpy, we get

$$\begin{aligned}
&\dot{U} = \dot{Q} + \dot{W} &(7)\\
&\implies \frac{D}{Dt}\int_{\Omega} HdV = -\int_{\partial\Omega} KT_{,j}(-n_j)ds + -\int_{\partial\Omega} \tau_{ij}u_i(-n_j)ds &(8)\\
&\implies \int_{\Omega} \frac{DH}{Dt}dV = \int_{\Omega} (KT_{,j} + \tau_{ij}u_i)_{,j}dV &(9)\\
&\implies \frac{DH}{Dt} = (KT_{,j})_{,j} + \tau_{ij}u_{i,j} &(10)
\end{aligned}$$

Equation 10 can be rewritten as

$$\frac{\partial H}{\partial t} + \underline{\mathrm{u}} \cdot \nabla H = K \nabla^2 T + \tau_{ij} \dot{\epsilon}_{ij} \tag{11}$$

in which the material derivative of enthalpy is the sum of the enthalpy flux and the work put into the system by deformation. Equation 11 is the conservation of energy equation, in which internal energy is a sum of change of energy from heat and the change in energy due to work being done on the volume. This balance relates the change in surface, strain, and thermal energy to the work rate. We can partition Equation 11 into:

$$\frac{c\gamma}{d} - \frac{1}{2}\left(\frac{D}{d}\right)^{\frac{p}{2}} \frac{\tau_s^2}{\mu} = (1 - \Theta)\tau_{ij}\dot{\epsilon}_{ij} \tag{12a}$$

$$\rho c_p \left(\frac{\partial T}{\partial t} + \underline{\mathrm{u}} \cdot \nabla T \right) = K \nabla^2 T + \Theta \tau_{ij} \dot{\epsilon}_{ij} \tag{12b}$$

where Equation 12a is the non-thermal energy component found from Equation 3 and Equation 12b is the thermal energy component (also known as the evolution of temperature equation). This relates the change in thermal energy (left hand side) to the change in heat through heat conduction and the change in heat that originates from viscous dissipation ($\Theta \tau_{ij} \dot{\epsilon}_{ij}$). For the purposes of ice-flow models, we generally neglect firn compaction, air movement through firn, and melting/refreezing. In the case of this model, we also neglect geothermal heat, as we are most interested in how heat generated during the deformation and movement of ice affects ice flow, since these may provide positive feedbacks that amplify the effects during ice flow. Meyer & Minchew (2018) previously derived a thermomechanical model from this energy balance to estimate ice temperature in shear margins of Antarctic ice streams. The study presented here follows their model and the assumptions from their model, including that there is no vertical shear. In other words, the strain rates are constant throughout the ice column and the ice slips along its bed. This implies that basal drag is negligible compared to drag along the lateral margins of the ice streams. Therefore, the primary heat source would be viscous dissipation during deformation.

While some fraction Θ of the mechanical work put into the ice during deformation gets converted into thermal energy, which is then advected or diffused, the remainder of the work gets converted into strain energy. Deformation increases the density of dislocations, which increases the strain energy state of ice (De La Chapelle et al., 1998). As the density of dislocations increases, the rate of deformation decreases due to pile-ups of dislocations preventing further creep (called work-hardening or strain-hardening) (Wilson & Zhang, 1996). Recovery mechanisms, including dynamic recrystallization, reduce the density of dislocations and allow for further creep. Recrystallization annihilates dislocations, either by the outward migration of grain boundaries, which destroy dislocations in their path (migration recrystallization), or by the subdivision of grains, during which new, strain-free grains are formed (rotation recrystallization) (Rollett & Kocks, 1993; Wenk et al., 1997; De Bresser et al., 1998; De La Chapelle et al., 1998; Montagnat & Duval, 2004).

Thus, during deformation, mechanical energy is converted to strain energy, and rotation recrystallization converts strain energy into surface energy, stored within grain boundaries (Derby & Ashby, 1987; Derby, 1992; De La Chapelle et al., 1998; Montagnat & Duval, 2000). Both mechanisms also destroy dislocation pileups, allowing dislocations to advect through dislocation creep, which functionally converts some of that strain energy back into mechanical energy. Finally, much of the strain energy is released during fracture events.

Therefore, as dislocations (and thus, strain energy) move with the strain-hardened ice downstream, eventually that energy is converted into surface energy during fracture and calving. We assume in this study that no other mechanisms are altering the energy state. It is unknown at the moment whether processes convert energy directly from surface and strain energy into heat, or whether all strain energy gets transferred back to mechanical energy or stored in grain boundaries or subgrain walls. Without further work suggesting otherwise, we assume this is not the case and reserve for future work an exploration of other mechanisms that may change the energy states.

However, the amount of mechanical energy converted to strain energy $(1 - \Theta)$ remains unknown. Constraining Θ is clearly necessary to fully understand the thermodynamics and energetics of ice flow and deformation, and thus the focus of this study is to constrain Θ.

2. Thermomechanical Model

Meyer & Minchew (2018) derived a thermomechanical model to compute ice temperature. Since their model only considered one column of ice, they simplified the heat equation to

$$-\rho c_p a \frac{\partial T}{\partial z} = K \frac{\partial^2 T}{\partial z^2} + \Theta \tau_{ij} \dot{\epsilon}_{ij} \tag{13}$$

where vertical velocity of ice $w = -a$ and lateral advection of ice is neglected. Note that they assumed $\Theta = 1$, and here we will rederive the model including this parameter Θ. The constitutive relation describing the flow of ice relates the stress to the strain rate as

$$\tau_{ij} = A^{\frac{-1}{n}} \left(\frac{1}{2} \dot{\epsilon}_{kl} \dot{\epsilon}_{kl} \right)^{\frac{1-n}{2n}} \tag{14}$$

where n is the exponent in the constitutive relation commonly taken to be $n = 3$, from borehole studies and laboratory measurements and A is the prefactor in the flow law, also known as the flow rate parameter. A describes the dependence of viscosity to a number of factors including temperature, fabric, porosity, liquid water content. From the constitutive relation, we can then approximate

$$\Theta \tau_{ij} \dot{\epsilon}_{ij} = 2\Theta A^{-\frac{1}{n}} \dot{\epsilon}^{\frac{n+1}{n}} \tag{15}$$

where $\dot{\epsilon}$ is the lateral shear strain rate. We can further define two nondimensional numbers: Brinkmann number represents the rate of dissipative heating to heat conduction:

$$Br = \frac{\Theta \tau_{ij} \dot{\epsilon}_{ij} H^2}{K \Delta T} \tag{16}$$

where ΔT is the difference between the melting temperature and the surface temperature, and the Peclet number represents the ratio of accumulation to diffusion and is found as

$$Pe = \frac{\rho c_p a H}{K} \tag{17}$$

where a is accumulation and H is ice thickness. The critical shear strain rate to form a temperate zone (a zone of temperate ice, heated by viscous dissipation) is

$$\dot{\epsilon}^* = \left(\frac{\frac{1}{2} Pe^2}{Pe - 1 + \exp\{-Pe\}} \right)^{\frac{n}{n+1}} \left[\frac{K \Delta T}{\Theta A^{\frac{-1}{n}} H^2} \right]^{\frac{n}{n+1}} \tag{18}$$

The thickness of this temperate zone is found by

$$\frac{\xi}{H} = \begin{cases} 1 - \frac{Pe}{Br} - \frac{1}{Pe}[1 + \mathcal{W}(-\exp\{-\frac{Pe^2}{Br} - 1\})], & \dot{\epsilon} > \dot{\epsilon}^* \\ 0, & \dot{\epsilon} \leq \dot{\epsilon}^* \end{cases} \tag{19}$$

where $f(\mathcal{W}) = \mathcal{W}e^{\mathcal{W}}$ is the product logarithm, i.e. the Lambert-W function. They then solve Equation 13 for ice temperature to find the following closed-form expression for ice temperature in the single column of ice:

$$T = \begin{cases} T_s + \Delta T \frac{Br}{2}[1 - \frac{z}{H} + \frac{1}{Pe}\exp\{Pe(\frac{\xi}{H} - 1)\} - \frac{1}{Pe}\exp\{Pe(\frac{\xi - z}{H})\}], & \xi \leq z \leq H \\ T_m, & 0 \leq z \leq \xi \end{cases} \tag{20}$$

The model defined by Equations 18, 19, 20 enables an estimate of ice temperature with depth, the existence of a temperate zone, and its thickness if one exists. Neither Meyer & Minchew (2018) nor our study accounts for geothermal heating in order to focus the study on the role of viscous dissipation, but it is feasible to represent the effects of geothermal heating through the boundary conditions of this thermomechanical model.

Meyer & Minchew (2018) apply this model to ice streams in Antarctica to show that active temperate zones may exist in many ice streams in Antarctica. However, we will recall that they assume $\Theta = 1$, thereby neglecting any other processes that may be resultant from the work done during ice deformation in shear margins. Here we seek to determine whether other processes may be significant and if this alters the estimates of ice temperature and temperate zones produced by Meyer & Minchew (2018), among other studies.

3. Steady State Grain Size Model

The steady-state grain size model was derived in Ranganathan et al. (2021) and follows the watt-meter derived by Austin & Evans (2007) and further explored and used by Behn et al. (2009, 2020). Steady-state grain size is found by assuming three recrystallization mechanisms - normal grain growth, rotation recrystallization, and migration recrystallization - operate independently such that (Austin & Evans, 2007)

$$\dot{d} = \dot{d}_{rot} + \dot{d}_{mig} + \dot{d}_{nor} \tag{21}$$

The change in grain size due to normal grain growth is typically parameterized by (Alley et al., 1986)

$$d^p_{\mathrm{nor}} = d^p_0 + kt \tag{22}$$

where d is grain size, d_0 is initial grain size, p is the grain-growth exponent, and k is the grain growth rate. Rotation and migration recrystallization recrystallization are both activated by deformation and alter surface and strain energy, respectively. Therefore, to find the change in grain-size, we can estimate the change in surface and strain energy that occurs as ice deforms. Rotation recrystallization alters the surface energy by subdividing grains, and therefore the change in surface energy due to rotation recrystallization is found by (Austin & Evans, 2007)

$$\dot{E}_{\mathrm{surface}} = \frac{-c\gamma}{d^2}\dot{d}_{rot} \tag{23}$$

where c is a geometric constant, d is grain-size, and γ is grain-boundary energy. Migration recrystallization alters strain energy by annihilating dislocations. The change in strain energy and grain size due to migration recrystallization is derived by Ranganathan et al. (2021) as

$$\dot{E}_{\text{strain}} = -\frac{1}{2}\frac{\tau_s^2}{\mu}\frac{p}{2}\frac{D^{\frac{p}{2}}}{d^{\frac{p}{2}+1}}\dot{d}_{mig} \tag{24}$$

$$\dot{d}_{\text{strain}} = MF_{mig} = \frac{1}{2}\frac{\tau_s^2}{\mu}\frac{D^{\frac{p}{2}}}{d^{\frac{p}{2}}}M \tag{25}$$

where τ is deviatoric shear stress, μ is the shear modulus, p is the grain-growth exponent, M is grain-boundary mobility, and D is a characteristic length-scale. Equations 23 and 24 can be applied to estimate $\dot{d}_{\text{rot}}$ by applying the equation for non-thermal energy found in Text S1 ($E_{\text{non-thermal}} = E_{\text{surface}} - E_{\text{strain}}$) and noting that $\dot{E}_{\text{non-thermal}} = (1-\Theta)\tau_{ij}\dot{\epsilon}_{ij}$. Then, we can apply this to Equation 21 to find steady-state grain size:

$$d_{ss} = \left[\frac{\overbrace{4kp^{-1}c\gamma\mu^2}^{\text{Normal grain growth}} + \overbrace{\tau_s^4 D^p\left(\frac{p}{2}\right)M}^{\text{Migration recrystallization}}}{\underbrace{8(1-\Theta)\tau_s\dot{\epsilon}_s\mu^2}_{\text{Rotation Recrystallization}}}\right]^{\frac{1}{1+p}} \tag{26}$$

4. Computing Θ

To accurately predict ice temperature, the presence of temperate zones, and grain-sizes in shear margins, we must constrain Θ, the fraction of deformational work that is dissipated as heat, to gather a more complete understanding of the energy budget in glacier shear margins. We consider the balance of energy density in a given control volume between thermal energy density, surface and grain-boundary energy density, and elastic strain energy density, such that Θ can be written as

$$\Theta(\dot{\epsilon}, D, p, n) = \frac{|\dot{E}_{\text{thermal}}(\Theta,\dot{\epsilon},n,T(\Theta,\dot{\epsilon},n))|}{|\dot{E}_{\text{thermal}}(\Theta,\dot{\epsilon},n,T(\Theta,\dot{\epsilon},n))| + |\dot{E}_{\text{surface}}(d(\Theta,\dot{\epsilon},D,p,n))| + |\dot{E}_{\text{strain}}(d(\Theta,\dot{\epsilon},D,p,n),D,p,T(\Theta,\dot{\epsilon},n} \tag{27}$$

where $\dot{E}_{\text{thermal}}$ represents the change in internal energy density due to change in thermal energy density due to viscous dissipation, $\dot{E}_{\text{surface}}$ represents the change in surface energy density due to the reduction in grain size during rotation recrystallization, and $\dot{E}_{\text{strain}}$ represents the change in elastic strain energy density due to migration recrystallization.

The increase in internal surface energy density due to the reduction in grain size is presented in Equation 23 and each of the terms are defined below. Note that during implementation, the rates of change are discretized ($\dot{E} \implies \Delta E$).

$$\dot{E}_{\text{surface}} = \frac{-c\gamma}{d^2}\dot{d}_{\text{rot}} \tag{28}$$

For example, for a discrete increase in grain size from about 2 mm at the surface to 40 mm at the bed, the magnitude of $\Delta E_{surface} \approx 10^3$ J m^{-3}. We approximate elastic strain energy from our interpretation of the dynamics occurring during migration recrystallization, so that that elastic strain energy density can be approximated by the change in energy due to an increase in dislocation density (Equation 24):

$$\dot{E}_{\text{strain}} = -\frac{1}{2}\frac{\tau_s^2}{\mu}\frac{D^{\frac{p}{2}}}{d^{\frac{p}{2}+1}}\dot{d}_{\text{mig}} \tag{29}$$

For a discrete increase in grain size from 2 mm to 40 mm, the magnitude of $\Delta E_{strain} \approx 10^7$ J m^{-3} for $\mu = 3e9$ Pa, $D = 0.05$ m, $p = 9$. Finally, the change in thermal energy density can be found by

$$\dot{E}_{\text{thermal}} = \rho_i c_p \dot{T} \tag{30}$$

Since for ice, $\rho_i \approx 917$ kg m^{-3} and $c_p \approx 2000$ J kg^{-1} K^{-1} (Giauque & Stout, 1936), for a discrete increase in temperature from 248 K to 273 K, the magnitude $\Delta E_{thermal} \approx 10^7$ J m^{-3}.

Since these internal energies are dependent upon temperature and grain size, which are both dependent upon Θ, Equation 27 becomes a nonlinear equation that is solved using the Trust-Region-Dogleg method.

4.1. Binary Behavior of Θ

In nearly every case of strain rate and n value, there are two distinct solutions for different p and D values, because in almost all cases, E_{surface} is much less than E_{strain} and in some cases E_{surface} is much less than E_{strain}. If these two criteria are true, we can rewrite Equation 27 as

$$\Theta = \left[1 + \frac{\Delta E_{\text{strain}}}{\Delta E_{\text{thermal}}}\right]^{-1} \tag{31}$$

Thus, when $\frac{\Delta E_{\text{strain}}}{\Delta E_{\text{thermal}}} << 1$, $\Theta = 1$ and otherwise, $\Theta < 1$. From Equations 29 and 30, $\Theta = 1$ when

$$\frac{-\frac{1}{2}\frac{\sigma_s^2}{\mu}\frac{D^{\frac{p}{2}}}{d^{\frac{p}{2}+1}}\Delta d}{\rho_i c_p \Delta T} << 1 \tag{32}$$

Considering general values of grain size ($\sim \mathcal{O}(10\text{mm})$), temperature ($\sim 255-270$K), shear modulus ($3 \times 10^9$ Pa), and stress ($\sim \mathcal{O}(10^5\text{Pa})$), this simplifies to $\Theta = 1$ when

$$(\frac{D}{d})^{\frac{p}{2}} << 10^7 \tag{33}$$

Equation 33 provides the basis for Θ being binary. When, for example, $p \approx 2$, Equation 33 holds and $\Theta = 1$ for all strain rates. However, when $p \approx 9$, $(\frac{D}{d})^{\frac{p}{2}} \approx 10^7$ and $\Theta < 1$. This binary behavior of Θ allows us to completely map the possible values of Θ in glacier shear margins by considering two cases: Regime A (in which $D = 0.05$ and $p = 2$) and Regime B (in which $D = 0.05$ and $p = 9$). These two regimes cover the possible values of Θ for varying values of D and p.

5. Estimates of Θ for a Full Parameter Space

Equation 26 gives a steady-state grain size model, dependent on the fraction of work that is dissipated as heat in deforming glacier ice (the parameter Θ). We use the thermo-mechanical model derived by Meyer & Minchew (2018) to compute ice temperature, with Θ accounted for in the Brinkmann number (the ratio of heating to conduction). Both models assume steady-state creep, and the full ice column of shear margins are likely in steady state due to the speed of deformation driving a short time (< 10 years) to steady state.

This parameter Θ is currently unknown but controls both the steady state ice temperature and the steady state grain size. Figure S1 presents profiles of ice temperature and grain size for varying Θ. We show the variation in temperature and grain size profiles for ranges of reasonable strain rates seen within Antarctic ice streams (excluding very large or very small strain rates).

The fraction Θ controls how much ice temperature increases with increasing strain rate and, consequently, how much grain sizes grow. The grain size at the bed is largely controlled by Θ, the characteristic length scale D, and the grain-growth exponent p. As Θ decreases, zones of temperate ice disappear and temperature and grain size profiles approach approximately constant values with depth ($\Theta = 0.01$). Furthermore, strain rates play a significant role in determining the magnitude of grain growth and temperature increases. For large strain rates (dotted lines), temperate zones remain quite large for smaller Θ and grains becomes coarse rapidly $\sim$ 30 mm. However, for low strain rates (dashed lines), grains remain roughly constant with temperature for all Θ and temperatures never reach the melting point, even for $\Theta = 0.99$. Finally, for moderate strain rates (solid lines), a zone of temperate ice forms for $\Theta = 0.99$ but for $\Theta <\sim 0.9$, the temperate zone disappears. The most dramatic grain growth occurs for moderate strain rates at approximately halfway down the ice column.

The rapid growth of grains is due to temperatures approaching $-10°$C, when enough strain energy has built for grain boundaries to migrate through migration recrystallization. Below approximately 500 meters height above the bed, grain sizes become roughly constant with depth, due to strain and temperature increasing enough such that creep and subsequent grain reduction due to rotation recrystallization becomes more active. Once ice temperature reaches the melting point and temperate zones form, recrystallization processes likely change due to the presence of significant liquid water in between grain boundaries. This liquid water likely makes grain boundaries even more mobile, encouraging coarsening of grains. Extremely coarse grains have been found in temperate glaciers (Tison & Hubbard, 2000), though further theoretical and experimental work is needed to consider in depth the effect that recrystallization may have on temperate ice.

The parameter Θ is dependent upon the values of D, the characteristic grain size, and p, the grain-growth exponent, as well as strain rate and n, the exponent in the constitutive relation. Figure S2 shows Θ for the full D-p parameter space, for varying strain rate and n.

The value of the flow-law exponent n describes the sensitivity of strain rates to stresses and generally corresponds to the mechanism of ice flow. Values higher than 3 suggest a dislocation-creep regime, in which ice flow occurs through line defects called dislocations (Goldsby & Kohlstedt, 1997). In an $n = 4$ regime, $\Theta = 1$ for high strain rates, suggesting that thermal energy is higher in magnitude than elastic strain energy for most cases except very high strain rates $\dot{\epsilon} \approx 10^{-8}$ s^{-1}, for large values of D (large characteristic length-scale for elastic strain energy), and for high values of p (large grain growth exponents). Thus, in an $n = 4$ regime, $\Theta < 1$ only for very rapidly deforming glaciers.

A constitutive relation with $n = 2$ corresponds to a flow regime in which the dominant creep mechanism is grain-boundary sliding (Goldsby & Kohlstedt, 1997). If $n = 2$, Θ becomes close to 0, suggesting very little heating, for almost all physically-reasonable strain rates. At very low strain rates ($\dot{\epsilon} \approx 10^{-10}$ s^{-1}), $\Theta \approx \frac{1}{5}$ for much of the parameter space, likely due to strain rates being so low that most deformation is not occurring. Values of the flow exponent closer to $n = 3$ more accurately describe a combination of dislocation creep and grain-boundary sliding, a mechanism that is grain-size dependent and generally occurs in fine-grained materials (Ashby, 1972).

Further, the boundary between the two regimes changes based on the value of n and the strain rate. In particular, for low strain rates, $\Delta E_{\text{elastic}}$ is low, and therefore it is not necessarily much greater than $\Delta E_{\text{surface}}$. Thus, the assumption made to simplify Equation 27 to Equation 31 does not necessarily hold. This results in a more diffuse boundary and less defined binary behavior.

6. Results for Other Outlet Glaciers

Results for Bindschadler and MacAyeal Ice Stream are found in Figure S3 and results for Byrd Glacier are found in Figure S4.

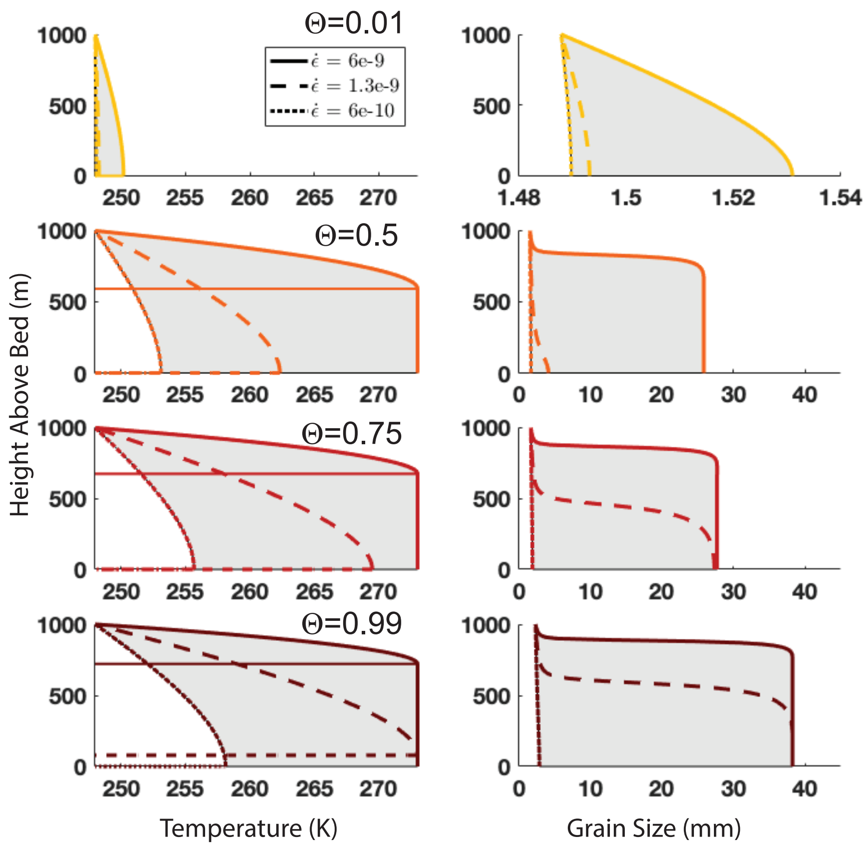

Figure S1. Ice temperature profiles, computed from the model derived in (Meyer & Minchew, 2018), and steady-state grain sizes profiles, computed from the model derived in this study, for varying values of Θ and varying lateral shear strain rates. A range of temperatures and grain sizes are plotted for low lateral shear strain rates ($\dot{\epsilon} = 6 \times 10^{-10}$ s^{-1}, dashed line), moderate strain rates ($\dot{\epsilon} = 1.3 \times 10^{-9}$ s^{-1}, solid line), and high strain rates ($\dot{\epsilon} = 6 \times 10^{-9}$ s^{-1}, dotted line). We use the constitutive relation to compute the work rate.

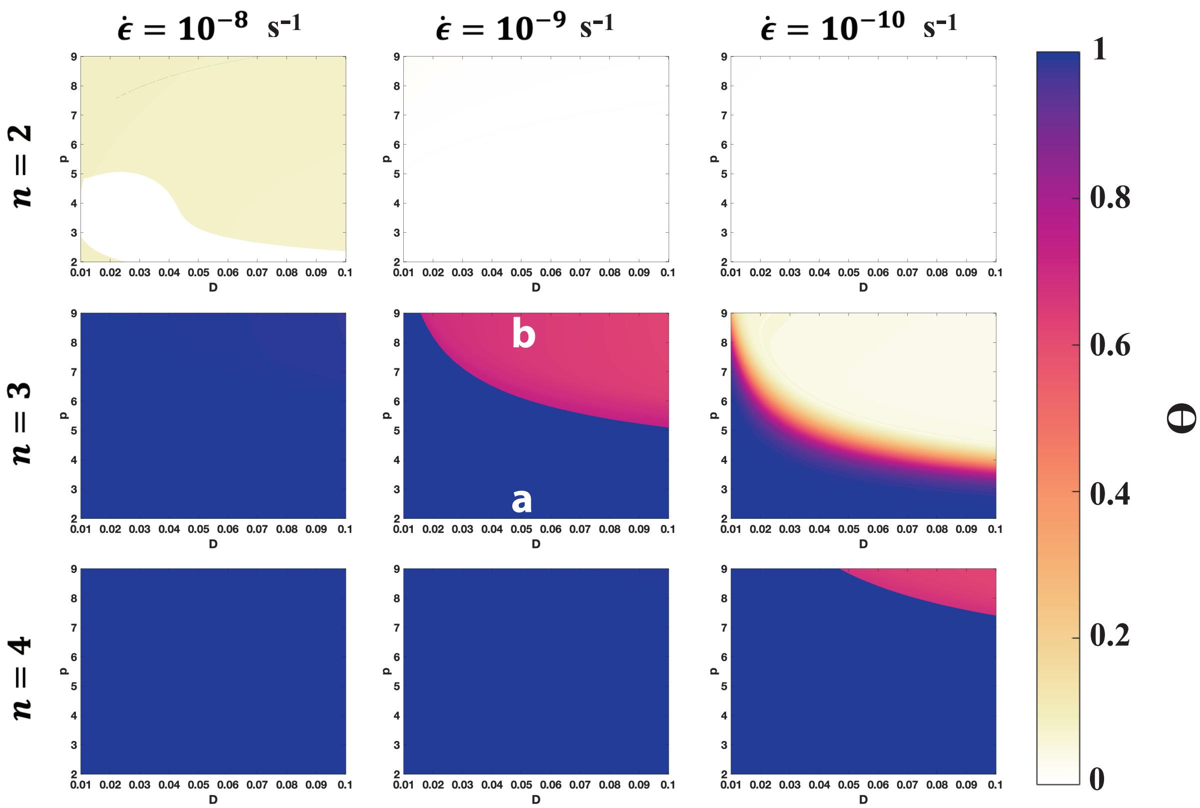

Figure S2. Estimated values of Θ for varying characteristic length scale for migration recrystallization, D, grain growth exponent, p, flow law exponent, n, and lateral shear strain rate. For most cases, there are two clear regimes for varying D and p, which we label Regime A and Regime B (middle panel).

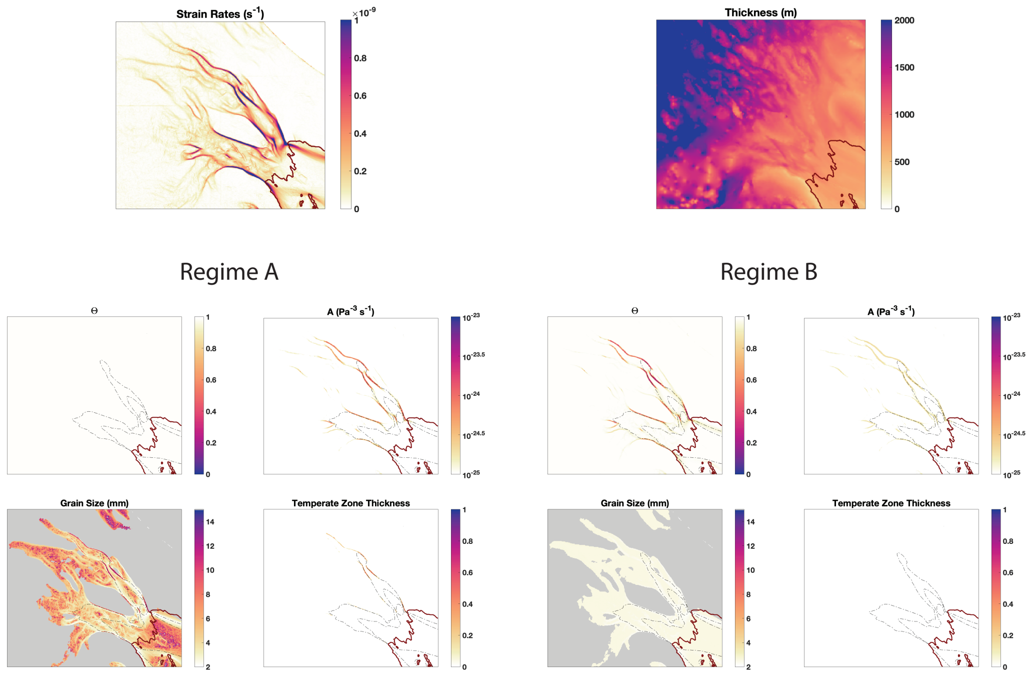

Figure S3. Strain rates computed from surface velocity fields derived from Landsat 7 and 8 (Gardner et al., 2018) and thickness computed from REMA surface elevation (Howat et al., 2019) and BedMachine bed topography (Morlighem et al., 2020) in the first row. Second and third rows show estimated values of Θ, the depth-averaged flow-rate parameter, steady-state depth-averaged grain size, and the thickness of temperate zones as a fraction of ice thickness in Bindschadler and MacAyeal Ice Streams for both regimes (Regime A: $D = 0.05$ mm, $p = 2$, Regime B: $D = 0.05$ mm, $p = 9$).

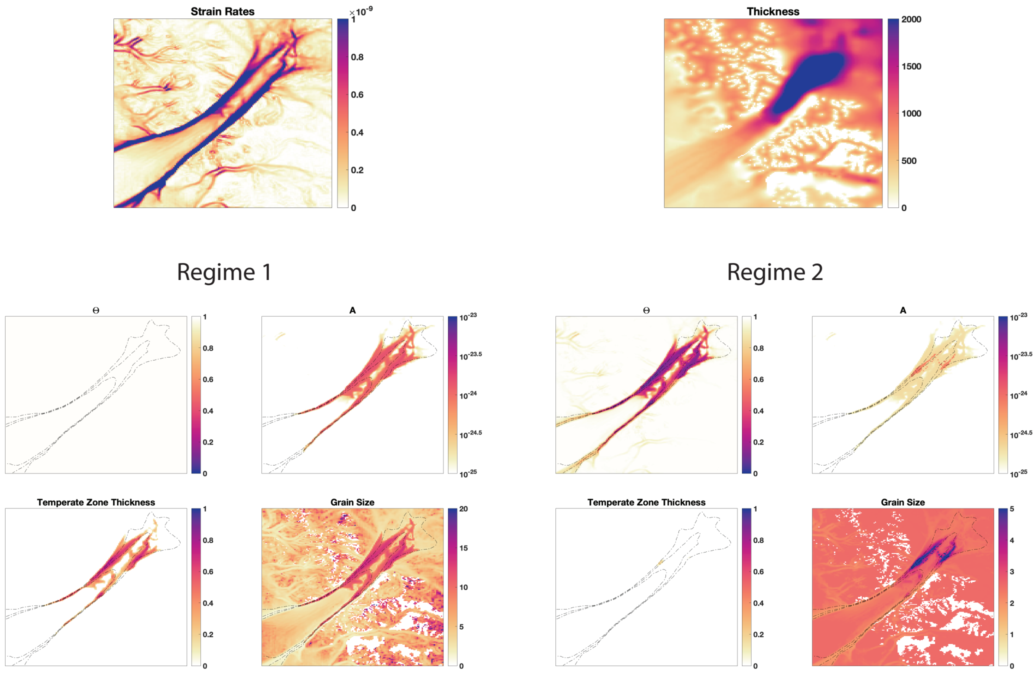

Figure S4. Strain rates computed from surface velocity fields derived from Landsat 7 and 8 (Gardner et al., 2018) and thickness computed from REMA surface elevation (Howat et al., 2019) and BedMachine bed topography (Morlighem et al., 2020) in the first row. Second and third rows show estimated values of Θ, the depth-averaged flow-rate parameter, steady-state depth-averaged grain size, and the thickness of temperate zones as a fraction of ice thickness in Byrd Glacier for both regimes (Regime A: $D = 0.05$ mm, $p = 2$, Regime B: $D = 0.05$ mm, $p = 9$).

References

Alley, R., Perepezko, J., & Bentley, C. (1986). Grain Growth in Polar Ice: I. Theory. *Journal of Glaciology*, *32*(112), 425–433. doi: 10.3189/s0022143000012132

Ashby, M. F. (1972). A first report on deformation-mechanism maps. *Acta Metallurgica*, *20*(7), 887–897. doi: 10.1016/0001-6160(72)90082-X

Austin, N. J., & Evans, B. (2007). Paleowattmeters: A scaling relation for dynamically recrystallized grain size. *Geology*, *35*(4), 343. Retrieved from `https://pubs.geoscienceworld.org/geology/article/35/4/343-346/129818` doi: 10.1130/G23244A.1

Behn, M. D., Goldsby, D. L., & Hirth, G. (2020). The role of grain-size evolution on the rheology of ice: Implications for reconciling laboratory creep data and the Glen flow law. *The Cryosphere Discussions*(November), 1–31. Retrieved from `https://tc.copernicus.org/preprints/tc-2020-295/` doi: 10.5194/tc-2020-295

Behn, M. D., Hirth, G., & Elsenbeck II, J. R. (2009, may). Implications of grain size evolution on the seismic structure of the oceanic upper mantle. *Earth and Planetary Science Letters*, *282*(1-4), 178–189. Retrieved from `http://dx.doi.org/10.1016/j.epsl.2009.03.014https://linkinghub.elsevier.com/retrieve/pii/S0012821X09001575` doi: 10.1016/j.epsl.2009.03.014

De Bresser, J. H. P., Peach, C. J., Reijs, J. P. J., & Spiers, C. J. (1998, sep). On dynamic recrystallization during solid state flow: Effects of stress and temperature. *Geophysical Research Letters*, *25*(18), 3457–3460. Retrieved from `http://doi.wiley.com/10.1029/98GL02690` doi: 10.1029/98GL02690

De La Chapelle, S., Castelnau, O., Lipenkov, V., & Duval, P. (1998, mar). Dynamic recrystallization and texture development in ice as revealed by the study of deep ice cores in Antarctica and Greenland. *Journal of Geophysical Research: Solid Earth*, *103*(B3), 5091–5105. Retrieved from http://doi.wiley.com/10.1029/97JB02621 doi: 10.1029/97JB02621

Derby, B. (1992, dec). Dynamic recrystallisation: The steady state grain size. *Scripta Metallurgica et Materialia*, *27*(11), 1581–1585. Retrieved from https://linkinghub.elsevier.com/retrieve/pii/0956716X92901488 doi: 10.1016/0956-716X(92)90148-8

Derby, B., & Ashby, M. (1987, jun). On dynamic recrystallisation. *Scripta Metallurgica*, *21*(6), 879–884. Retrieved from https://linkinghub.elsevier.com/retrieve/pii/0036974887903413 doi: 10.1016/0036-9748(87)90341-3

Gardner, A. S., Moholdt, G., Scambos, T., Fahnstock, M., Ligtenberg, S., van den Broeke, M., & Nilsson, J. (2018, feb). Increased West Antarctic and unchanged East Antarctic ice discharge over the last 7 years. *The Cryosphere*, *12*(2), 521–547. Retrieved from https://tc.copernicus.org/articles/12/521/2018/ doi: 10.5194/tc-12-521-2018

Giauque, W. F., & Stout, J. W. (1936, jul). The Entropy of Water and the Third Law of Thermodynamics. The Heat Capacity of Ice from 15 to 273K. *Journal of the American Chemical Society*, *58*(7), 1144–1150. Retrieved from https://pubs.acs.org/doi/abs/10.1021/ja01298a023 doi: 10.1021/ja01298a023

Goldsby, D. L., & Kohlstedt, D. L. (1997). Flow of ice by Dislocation, Grain Boundary Sliding, and Diffusion Processes. *Lunar and Planetary Science*.

Howat, I. M., Porter, C., Smith, B. E., Noh, M.-J., & Morin, P. (2019, feb). The Reference Elevation Model of Antarctica. *The Cryosphere*, *13*(2), 665–674. Retrieved from https://tc.copernicus.org/articles/13/665/2019/ doi: 10.5194/tc-13-665-2019

Meyer, C. R., & Minchew, B. M. (2018, sep). Temperate ice in the shear margins of the Antarctic Ice Sheet: Controlling processes and preliminary locations. *Earth and Planetary Science Let-*

ters, *498*, 17–26. Retrieved from `https://doi.org/10.1016/j.epsl.2018.06.028https://linkinghub.elsevier.com/retrieve/pii/S0012821X18303790` doi: 10.1016/j.epsl.2018.06.028

Montagnat, M., & Duval, P. (2000, nov). Rate controlling processes in the creep of polar ice, influence of grain boundary migration associated with recrystallization. *Earth and Planetary Science Letters*, *183*(1-2), 179–186. Retrieved from `https://linkinghub.elsevier.com/retrieve/pii/S0012821X00002624` doi: 10.1016/S0012-821X(00)00262-4

Montagnat, M., & Duval, P. (2004). Dislocations in ice and deformation mechanisms: From single crystals to polar ice. *Defect and Diffusion Forum*, *229*(January 2017), 43–54. doi: 10.4028/www.scientific.net/ddf.229.43

Morlighem, M., Rignot, E., Binder, T., Blankenship, D., Drews, R., Eagles, G., ... Young, D. A. (2020). Deep glacial troughs and stabilizing ridges unveiled beneath the margins of the Antarctic ice sheet. *Nature Geoscience*, *13*(2), 132–137. Retrieved from `http://dx.doi.org/10.1038/s41561-019-0510-8` doi: 10.1038/s41561-019-0510-8

Ranganathan, M., Minchew, B., Meyer, C., & Pec, M. (2021). *Recrystallization of ice enhances the creep and vulnerability to fracture of ice shelves.* doi: 10.31223/X5W31W

Rollett, A. D., & Kocks, U. (1993). A Review of the Stages of Work Hardening. *Solid State Phenomena*, *35-36*(January), 1–18. doi: 10.4028/www.scientific.net/ssp.35-36.1

Tison, J. L., & Hubbard, B. (2000). Ice crystallographic evolution at a temperate glacier: Glacier de Tsanfleuron, Switzerland. *Geological Society Special Publication*, *176*, 23–38. doi: 10.1144/GSL.SP.2000.176.01.03

Wenk, H. R., Canova, G., Bréchet, Y., & Flandin, L. (1997). A deformation-based model for recrystallization of anisotropic materials. *Acta Materialia*, *45*(8), 3283–3296. doi: 10.1016/

S1359-6454(96)00409-0

Wilson, C. J., & Zhang, Y. (1996). Development of microstructure in the high-temperature deformation of ice. *Annals of Glaciology*, *23*, 293–302. doi: 10.3189/s0260305500013562